

IFSCC 2025 full paper (IFSCC2025-462)

## **Effects of Extracellular Vesicles on Skin Aging Biomarkers in a 3D Reconstructed Skin Model**

**Yao TENG<sup>1</sup>, Sarah GIRARDEAU-HUBERT<sup>2</sup>, Benedicte FALLOU<sup>3</sup>, Richard BETTS<sup>4</sup>, Franck JUCHAUX<sup>2</sup>, Xavier MARAT<sup>2</sup>, Rodrigo De VECCHI<sup>2</sup>, Ping WANG<sup>1</sup>, Nan HUANG<sup>1</sup>, Daniel ROY<sup>5</sup>, Yu GAO<sup>1</sup> and Qian ZHENG<sup>5</sup>**

<sup>1</sup> Advanced Research, L'Oréal Research & Innovation, Shanghai, China; <sup>2</sup> Advanced Research, L'Oréal Research & Innovation, Aulnay-sous-Bois, France; <sup>3</sup> EPISKIN, L'Oréal Research & Innovation, Lyon, France; <sup>4</sup> Advanced Research, L'Oréal Research & Innovation, Singapore; <sup>5</sup> Advanced Research, L'Oréal Research & Innovation, Clark, New Jersey, United States;

### **1. Introduction**

Bio-based materials, including platelet rich plasma (PRP) [1], extracellular vesicles (EVs) [2], stromal vascular fraction (SVF) [3] and a range of isolated growth factors [4], are emerging technologies for tissue regeneration [5], promoting cell proliferation, differentiation, migration, angiogenesis, and matrix remodeling [6-9]. EVs are natural vesicles mediating intercellular communication [10], making them promising therapeutic candidates for treating tissue ageing, enhancing regenerative aesthetics, and addressing scar & burns [11, 12]. EVs consist of a phospholipid bilayer and can carry a diverse array bioactive components including proteins, nucleic acids, and lipids [13]. The cargo and subsequent bioactivity of EVs is a function of the cell from which they are derived; moreover, EVs have distinct characteristics compared to their parental cells that are favorable for clinical use, such as the inability to self-replicate, reduced immunogenicity, and improved transportability and storage [12]. There are several examples in recent literature demonstrating the regenerative potential of EVs from various cell sources, including fibroblasts, platelets, adipose-derived stem cells (ADSCs), umbilical cord-derived mesenchymal stem cells (UC-MSCs), and bone marrow [14, 15]. These data are primarily from 2D *in vitro* and pre-clinical models.

To date, clinical data supporting the skin aesthetic and regeneration benefits of EVs remain limited. A double-blind trial showed improved acne scars reduction, reduced erythema and shorter downtime with ADSC-EVs combined with fractional CO<sub>2</sub> laser treatment [16]. Another study demonstrated the safety and efficacy of a topical platelet-derived exosome serum for reducing redness and improving skin health [17]. While several ongoing clinical studies are assessing EVs for wound healing (ClinicalTrials.gov: NCT05475418) and anti-aging

(ClinicalTrials.gov: NCT05813379) applications, no EV products have received full approval by the US Food and Drug Administration.

While there is increasing evidence of the positive impact of mammalian EVs on skin diseases and skin regeneration, there remains considerable gaps in knowledge of EV efficacy and mechanisms of action. Traditional 2D cell assays lack crucial elements of cell-cell interactions and are unable to examine endpoints related to three-dimension structure, while animal studies struggle to faithfully replicate human skin physiology. Available clinical data on EVs comes with challenges in decoding mechanisms of action. *In vitro* 3D models offer several advantages in that they are reproducible, allowing for the study of human cells in a 3D microenvironment, and can be processed for a variety of biomarkers to gain mechanistic insights. Within the present study, we utilized 3D organotypic skin models, encompassing both epidermis and dermis, reconstructed with primary human cells to circumvent the limitations of many existing published approaches. These 3D models are shown to provide unique insights on the potential of bio-derived materials, including EVs from ADSCs and UC-MSCs, in promoting skin regeneration.

## 2. Materials and Methods

### 2.1 EV isolation and characterization

ADSCs and UC-MSCs were subjected to a phosphate-buffered saline (PBS) rinse and cultured in serum-free medium for 48 hours. The conditioned medium was collected to isolate EVs, with ultracentrifugation and filtration performed by Echo Biotech (Beijing, China). Size and particle count of EVs within vesicle suspensions were examined using the Zeta View PMX 110 (Particle Metrix, Meerbusch). Vesicles were visualized and photographed using a transmission electron microscope (H-7650, Hitachi Ltd.). Biomarkers of EVs were detected via western blot analysis using the following antibodies: rabbit polyclonal antibodies against human CD63 (sc-5275, Santa Cruz), CD9 (60232-Ig, Proteintech), HSP90 (60318-Ig, Proteintech), Alix (sc-53540, Santa Cruz), TSG101 (sc-13611, Santa Cruz), and calnexin (10427-2-AP, Promega).

### 2.2 Cell culture and fibroblast proliferation assay

Normal human fibroblasts (NHF) were obtained from surgical waste with informed written patient consent with ethics approval from the review board of the Skin Research Institute of Singapore. The NHF cells seeded into 96-well plates in medium containing 10% FBS. After 24h incubation, the medium was changed to 2% FBS, with or without treatment, including a 10% FBS positive control. After 3 days, cell proliferation was assessed using the CyQuant kit (Invitrogen, C35006), measured using a plate reader (SpectraMax, Molecular Devices). The cell stimulation range was normalized to 100% for cells treated with 10% FBS versus 2% FBS, and the stimulation ratio of EV-treated groups was calculated relative to this baseline.

### 2.3 Cellular uptake of EVs

EVs were labeled using the CM-Dil red fluorescent membrane linker dye (C7000, Invitrogen), following the manufacturer's guidelines. NHF cells were then exposed to CM-Dil-labeled EVs at a concentration of 100 µg/mL for a duration of 12 h. Subsequently, NHF cells underwent three washes with PBS, were fixed in 4% paraformaldehyde, and were stained with DAPI.

Finally, cellular uptake of the labeled EVs was observed using a Zeiss Confocal LSM 710 microscope.

#### **2.4 Full-thickness skin equivalent model**

The reconstructed skin models employed in this study were produced following established procedures [18]. Primary cells were isolated from surgical waste with informed written patient consent and ethical approval from the review board of the Skin Research Institute of Singapore. In summary, the dermal compartment was formed using a blend of collagen and dermal fibroblasts. Normal human keratinocytes (NHK) were subsequently seeded onto this layer on day 5. These models were incubated in a submerged environment using appropriate culture media for a duration of 7 days. Following this period, the skin tissue was transitioned to an air-liquid interface culture for an additional 7 days before being harvested.

#### **2.5 Optical Coherence Tomography (OCT) imaging and quantitative processing**

To obtain cross-sectional views of the human full thickness skin model, OCT (Thorlabs, Newton) was utilized. Optical imaging was performed using a 3D scan volume measuring  $9.42 \times 9.42 \times 1.5$  mm, comprising 512 X-Z slices for each sample. The thickness of the epidermal layer was quantified by Image J (NIH, Bethesda), based on optical images obtained via OCT. The average thickness was determined by calculating the area of the whole epidermal layer and its corresponding length.

#### **2.6 Histology and immunofluorescent (IF) staining**

The full thickness skin model was punched out into 10 mm-diameter punches for histological analysis and IF staining. Half of the punched samples were formaldehyde-fixed, paraffin-embedded, sectioned, and hematoxylin and eosin stained. The other half were O.C.T compound-embedded, cryosectioned, and acetone-fixed. Sections were blocked with 0.2% BSA and incubated with primary antibodies against human Ki67 (M7240, mouse, Dako), Collagen IV (MAB1430, mouse, Sigma), and Fibrillin 1 (1405-01, mouse, Southern Biotech). After washing, sections were incubated with Alexa Fluor 488 secondary antibody (A21202, Invitrogen), DAPI stained (D1306, Invitrogen), and imaged using a Nikon Eclipse Ti fluorescence microscope.

#### **2.7 Bulk transcriptomics analysis**

For full-thickness skin model RNA-seq, total RNA from 5-6 replicates per condition was extracted using the Qiagen RNeasy Mini Kit. Library preparation and sequencing (Illumina, TruSeq Stranded Total RNA kit) were performed by Shanghai Biotechnology Corporation (Shanghai, China). Differentially expressed genes (DEGs; fold change  $>1.5$  or  $<0.67$ ,  $p < 0.05$ ) were identified using EdgeR, and pathway enrichment analysis was conducted using the ClusterProfiler in the R language (version 3.6.2).

#### **2.8 Data Analysis**

Fluorescent images were processed using Image J. Statistical analysis (GraphPad Prism) is presented as mean  $\pm$  standard deviation unless otherwise specified. ANOVA with Dunnett's post-hoc test was used for group comparisons. Significant differences: \* $p < 0.05$ , \*\*  $p < 0.01$ .

### **3. Results**

### 3.1 Characterization of EVs isolated from ADSCs and UC-MSCs

EVs from ADSC and UC-MSCs underwent characterization in accordance with the MISEV2023 guidelines [19]. Consistent with the previous reports [20, 21], nanoparticle tracking analysis (NTA) showed the average diameter ( $\pm$  SD) of the ADSC EVs and UC-MSC EVs were  $125 \pm 5$  nm and  $130 \pm 7$  nm, respectively (Figure 1a). Transmission electronic microscopy (TEM) revealed that both ADSC and UC-MSC EVs exhibited round and cup-shaped structures, intact membrane structures, and a similar size range of approximately 100-200 nm in diameter as detected via NTA (Figure 1b). To further validate the EV identity, western blotting confirmed the presence of EV internal protein markers TSG101, HSP70 and surface protein marker CD63 in both the ADSC EVs and UC-MSC EVs. The negative marker endoplasmic reticulum calnexin, which should be expressed in the cell lysate (CL) group and was not expressed in the ADSC EVs and UC-MSC EVs (Figure 1c).

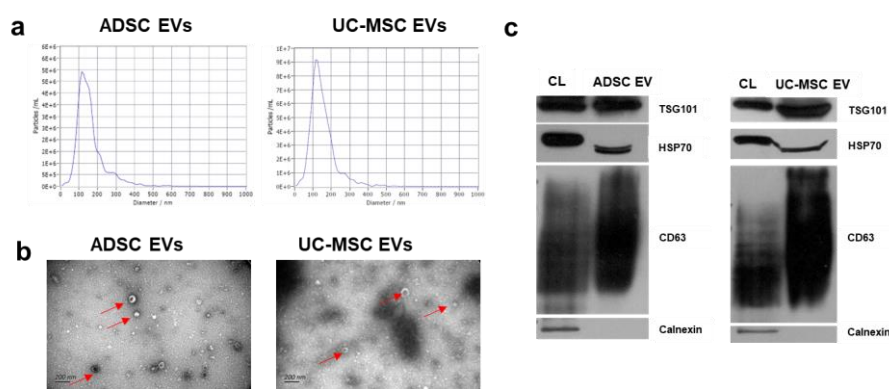


**Figure 1.** Characterization of ADSC EVs and UC-MSC EVs. (a) Size and concentration measurement by NTA; (b) EV morphology visualization (red arrows) with TEM. Scale bar, 200 nm; (c) EV related biomarkers confirmed with Western Blot, including positive markers TSG101, HSP70, CD63 and negative marker calnexin.

### 3.2 ADSC EV and UC-MSC EV effect on 2D fibroblasts

Normal human fibroblasts cultured in 2D were treated with ADSC EVs and UC-MSC EVs to investigate the impact of EVs on fibroblast proliferation. Treatment with  $1 \times 10^{10}$  particles/ml ADSC EVs led to 37% increase in cell proliferation, with a sustained 18% increase observed at lower test doses relative to controls (Figure 2b). UC-MSC EVs stimulated fibroblast proliferation at concentrations at or above  $1 \times 10^9$  particles/ml, culminating in a 23% increase in fibroblast proliferation at  $1 \times 10^{10}$  particles/ml. Unlike ADSC EVs,  $3 \times 10^8$  particles/ml of UC-MSC EVs did not yield an increase in cell proliferation (Figure 2c). Labeled ADSC and UC-MSC EVs were also shown to be internalized by fibroblasts (Figure 2d-e).

### 3.3 ADSC EV and UC-MSC EV effect on 3D skin reconstructed model

To examine the biological activity of EVs within a reconstructed skin system, the culture media of a human full thickness reconstructed skin model was administered ADSC EVs and UC-MSC EVs on Day 15, after the model was raised from the air-liquid interface. Culture medium containing the indicated treatment was renewed on Day 18 and incubated an additional 3 days. On Day 21, the models were harvested for various analyses, including OCT imaging, H&E staining, and IF staining (Figure 3a). The thickness of the epidermal layer within the skin

models was assessed and normalized relative to the untreated group. The application of Vitamin C served as a positive control and resulted in a significant increase in the thickness of the full epidermis (Figure 3c). ADSC EV- and UC-MSC EV-treated models exhibited marked enhancements in epidermal thickness at both EV concentrations, as determined by OCT (Figure 3c and 3e) and H&E staining (Figure 3d and 3f), with the latter measuring living cell layers. Moreover, the basal layer of the epidermis exhibited a higher degree of proliferation and polarization, characterized by elongated columnar basal keratinocytes oriented perpendicular to the dermo-epidermal junction (DEJ), compared to the cuboidal basal keratinocytes in the untreated groups (Figure 3d, yellow arrows).

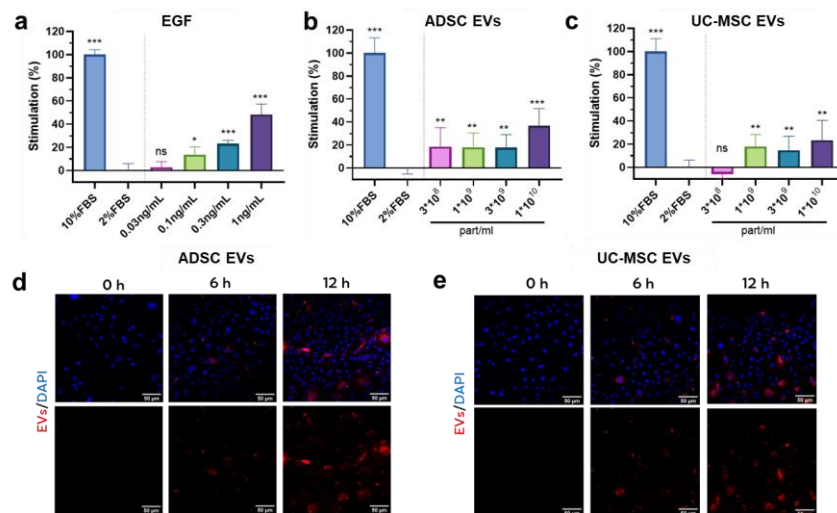


**Figure 2.** EV effect on 2D NHF cells. (a-c) 2D NHF proliferation regulated by EVs; (d-e) EV uptake in fibroblasts. One-way ANOVA, \*p<0.05, \*\*p<0.01, \*\*\*p<0.001. Data are representative of three independent experiments each performed in triplicate.

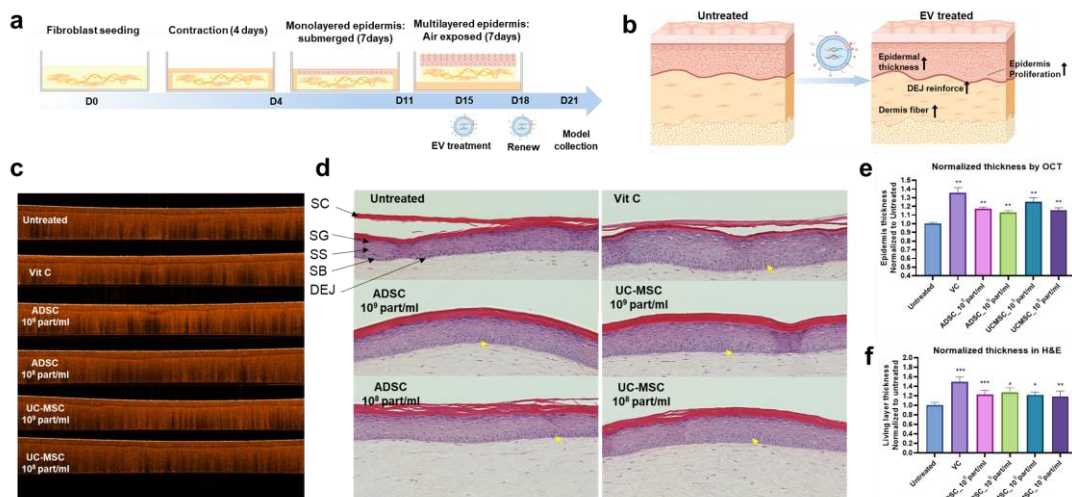


**Figure 3.** EV effect on epidermal layer in 3D reconstructed skin model. (a) Schematic diagram showing the experimental flow for human full thickness skin model with EV treatment, (b) focusing on related key marker changes (created with BioRender.com). (c) OCT images of the 3D skin models treated with or without EVs at different concentrations. (d) H&E staining of the skin model section treated with or without different EVs conditions. Quantitative results of the (e) epidermal thickness based on OCT and (f) the

thickness of the living cell layers based on H&E images. One-way ANOVA, \* $p<0.05$ , \*\* $p<0.01$ , \*\*\* $p<0.001$  versus Untreated. n=3, representative of 3 independent experiments each performed in triplicate.

Proliferating keratinocytes in the basal layer of the epidermis were visualized via immunostaining with a Ki67 antibody, a key marker of cellular proliferation. The fraction of Ki67-positive keratinocytes in the viable layers of the epidermis was quantified. Human full thickness skin models demonstrated that ADSC EV treatment at high and low concentrations resulted in a two-fold increase and a 1.9-fold increase in keratinocytes expressing Ki67, respectively. Treatment with UC-MSC EVs similarly resulted in 1.8 and 1.6-fold increases in Ki67 expression for high and low concentrations, respectively (Figure 4a).

The DEJ biomarker Collagen IV, which is part of the intricate network of extracellular matrix proteins that connect the two skin compartments and serves important regulatory functions, was also examined [18]. Collagen IV expression in the human full thickness skin model following treatment with 200  $\mu$ M vitamin C resulted in a significant 49% increase compared to the untreated control. The models treated with EVs derived from both ADSCs and UC-MSCs exhibited significantly elevated collagen IV expression, revealing approximate 45% increase with high concentrations of ADSC EVs and UC-MSC EVs. For ADSC EVs and UC-MSC EVs testing at low concentrations, there was an increase of 26% that fell short of reaching statistical significance.

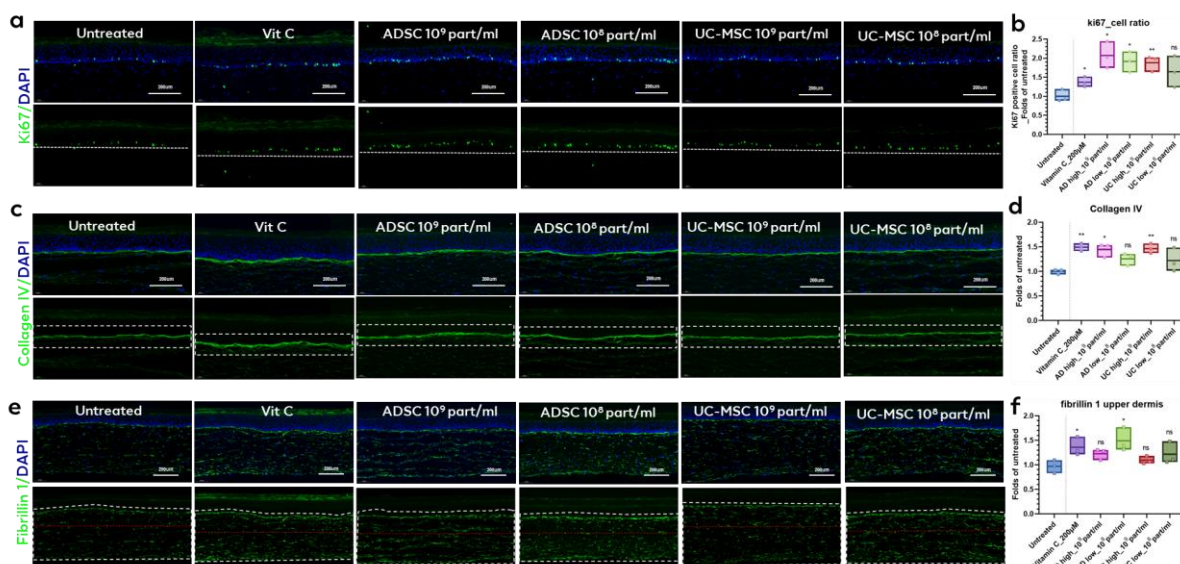


**Figure 4.** EV effects on skin biomarkers in 3D reconstructed skin model. (a) IF images for ki67 in skin model sections with different EV treatment conditions and (b) quantitative results for ki67-expressing cell ratio. (c) IF images for Collagen IV in skin model section with or without different EV treatment conditions and (d) quantitative results for collagen IV expression. (e) IF images for fibrillin 1 in skin model section with different EV treatment conditions and (f) quantitative results for fibrillin 1 expression. One-way ANOVA, \* $p<0.05$ , \*\* $p<0.01$ , \*\*\* $p<0.001$  versus Untreated. n=3, representative of 3 independent experiments.

Fibrillin 1 was also assessed, which is a structural glycoprotein to which tropoelastin molecules attach, forming elastin fibers in dermal layers. Expression of fibrillin 1 in human full thickness skin model was measured following treatment with 200  $\mu$ M vitamin C, resulting in a significant 36% increase compared to the untreated control, consistent with previous reports [29]. Expression of fibrillin 1 showed a 49% increase by ADSC EVs at  $10^8$  particles/ml, while the effect size at  $10^9$  particles/ml appeared to be less potent (23% increase,  $p=0.055$  vs. vehicle control). In parallel, an elevation of fibrillin 1 expression was observed for the UC-MSC EV groups at  $10^9$  particles/ml and  $10^8$  particles/ml (Figure 4f); however, these increases were not statistically significant. Notably, fibrillin 1 expression of EV-treated tissues exhibited a more elongated fiber-like structure.

### 3.4 Decoding ADSC and UC-MSC EV mechanisms for skin regeneration with transcriptomic analysis in 3D models

To gain more insight into the underlying mechanism for EVs in 3D models, the human full thickness skin models with and without the addition of ADSC EVs and UC-MSC EVs underwent lysis and were subjected to bulk transcriptomics analysis. This analysis revealed differentially expressed genes (DEGs) in human full thickness skin models treated with high and low concentrations of both EV types. Due to inter-model variability, overlapping DEGs from both concentrations were used, identifying 45 common DEGs across all EV treatments (Figure 5a). For the ADSC EV-treated group, 145 genes were found to be altered by both high and low testing concentrations, comprising 62 up-regulated and 83 down-regulated genes. The gene alteration profile of ADSC EV-treated group was illustrated with heatmap in Figure 5b, with distinct differences in clustering for EV-treated groups and untreated groups. Compared with the untreated models, UC-MSC EV-treated group showed 165 DEGs, comprising 58 up-regulated and 107 down-regulated genes (Figure 5c).

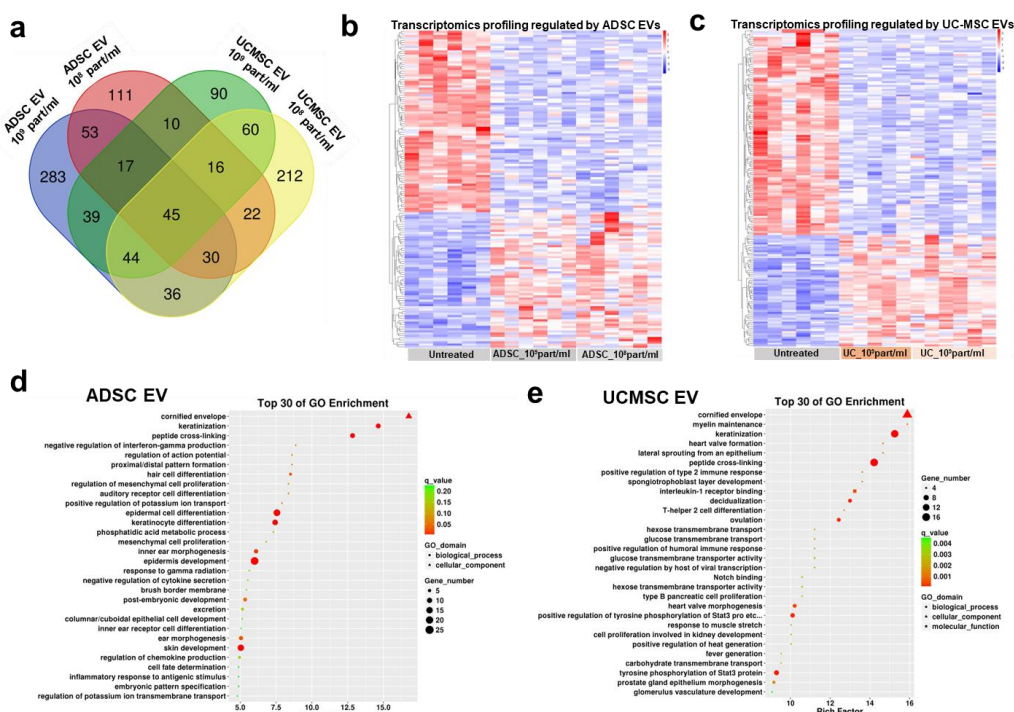


**Figure 5.** Bulk transcriptomics of reconstructed skin model following addition of ADSC EVs and UC-MSCs. (a) Venn plot of the DEGs identified with treatment of ADSC EVs and UC-MSC EVs. Heatmap of the common DEGs regulated by (b) ADSC EVs and (c) UC-MSC EVs at high and low doses, with 5–8 replicates for each testing group; (d, e) The DEGs regulated by ADSC EVs and UC-MSC EVs were enriched in GO database.

The DEGs from the skin models were further subjected to Gene Ontology (GO) analysis, and their enrichment profiles are depicted in Figure 5 d-e. Following ADSC EV addition, the DEGs were enriched in biological processes related to the upregulation of keratinization, epidermal cell differentiation, stem cell proliferation, and skin epidermis development. Similarly, the skin models treated with UC-MSC EVs displayed upregulated genes associated with stem cell proliferation, epidermal cell differentiation, and cell-substrate adhesion. Furthermore, the DEGs for skin models treated with either type of EV had downregulated genes correlated with inflammatory responses (e.g., IL-6) and genes linked to type 2 immune response, suggestive of the anti-inflammatory effect of EVs on the skin models. Notably, fewer genes and pathways related to dermis were identified compared to those related to epidermis, which may be attributed to the higher number of keratinocytes compared to fibroblasts in the reconstructed skin models.

#### 4. Discussion

Given limited clinical data on EV efficacy towards skin, the present study focused on ADSC and UC-MSC EVs, previously shown to have regenerative behaviors in 2D and pre-clinical tests. Consistent with prior studies [14, 22], ADSC EVs and UC-MSC EVs both increased fibroblast proliferation in 2D assays conducted herein. However, such 2D assays with a single cell-type are not completely predictive of how EVs would perform in 3D, multi-cell and differentiated systems. The human full thickness skin model enables the exploration of epidermal maturation, differentiation, and potential crosstalk with an underlying model dermis [18, 23]. In human full thickness skin model, both EV types significantly enhanced epidermal thickness, keratinocyte proliferation, and collagen IV expression. Specifically, evaluation of collagen IV, a DEJ marker, in the 3D human full thickness model addresses limitations of conventional 2D assays. Transcriptomics analysis revealed upregulated genes related to skin regeneration and downregulated inflammation-related genes. This finding is consistent with previous studies demonstrating that MSC EVs can decrease the expression of pro-inflammatory cytokines (e.g., IL-6, IL-1 $\beta$ , TNF- $\alpha$ ) [24], while increasing the expression of anti-inflammatory cytokines (e.g., IL-10) to facilitate skin repair [25, 26]. Although prior studies highlighted differences between EV sources [22], the observation from the current human full thickness skin model identifies several outcomes (e.g., epidermal thickness) similarly impacted by both ADSC and UC-MSC EVs.

EV structure and function are influenced by cell source, culture conditions, harvesting period, and isolation methods [27, 28]. Technologies like cell preconditioning, 3D bioreactor culture, physical or chemical stimulation, genetic manipulation, and hypoxia are under exploration to generate unique EVs [25, 29]. Isolation methods such as size exclusion chromatography and ultracentrifugation can also influence the EV yield and composition. Comprehensive

characterization is crucial, and although this study used standardized production and characterization procedure (MISEV2023 guidelines), results are not generalizable to all ADSC or UC-MSC EVs due to production variability.

The need for standardized EV evaluation is important, especially with the increasing demand for non-animal testing methods in cosmetics. 3D human skin equivalents offer a more physiologically relevant alternative to 2D cell cultures. This study used both 2D cells and 3D human full thickness skin models, which collectively supported a detailed understanding of skin-related biomarkers linked to regenerative processes for the EVs assessed here. Nevertheless, the pivotal findings related to efficacy and underlying mechanisms from these models necessitate validation through clinical studies, complemented by thorough safety and regulatory assessments.

## 5. Conclusion

In this study, EVs from ADSCs and UC-MSCs were quantified and characterized, with each EV possessing established EV biomarkers. The efficacy of the EVs was established through *in vitro* evaluation using skin cells and full-thickness skin models, revealing several noteworthy effects including increased fibroblast proliferation in 2D, and increased epidermal thickness, keratinocyte proliferation, and elevated collagen IV in the DEJ of human full thickness skin models. To gain insights into the molecular mechanisms underlying these effects, bulk transcriptomics was performed on the 3D reconstructed skin models, providing a comprehensive view of the gene expression profiles modulated by the EVs. Overall, this study expanded on previous literature establishing the pro-regenerative potential of EVs and emphasized the use of 3D reconstructed skin models as relevant and reproducible tools to assess aging-related biomarkers.

## Reference

1. Alsousou, J., et al., *The role of platelet-rich plasma in tissue regeneration*. Platelets, 2013. **24**(3): p. 173-82.
2. Lee, J.Y. and H.S. Kim, *Extracellular Vesicles in Regenerative Medicine: Potentials and Challenges*. Tissue Eng Regen Med, 2021. **18**(4): p. 479-484.
3. Bora, P. and A.S. Majumdar, *Adipose tissue-derived stromal vascular fraction in regenerative medicine: a brief review on biology and translation*. Stem Cell Research & Therapy, 2017. **8**(1): p. 145.
4. Ren, X., et al., *Growth Factor Engineering Strategies for Regenerative Medicine Applications*. 2020. **7**.
5. Crowley, J.S., A. Liu, and M. Dobke, *Regenerative and stem cell-based techniques for facial rejuvenation*. Exp Biol Med (Maywood), 2021. **246**(16): p. 1829-1837.
6. Davies, O.G., S. Williams, and K. Goldie, *The therapeutic and commercial landscape of stem cell vesicles in regenerative dermatology*. Journal of Controlled Release, 2023. **353**: p. 1096-1106.
7. Brunet, A., M.A. Goodell, and T.A. Rando, *Ageing and rejuvenation of tissue stem cells and their niches*. Nature Reviews Molecular Cell Biology, 2023. **24**(1): p. 45-62.
8. Ji, S., et al., *Cellular rejuvenation: molecular mechanisms and potential therapeutic interventions for diseases*. Signal Transduction and Targeted Therapy, 2023. **8**(1): p. 116.
9. Iismaa, S.E., et al., *Comparative regenerative mechanisms across different mammalian tissues*. npj Regenerative Medicine, 2018. **3**(1): p. 6.

10. Liang, X., et al., *Paracrine mechanisms of mesenchymal stem cell-based therapy: current status and perspectives*. Cell Transplant, 2014. **23**(9): p. 1045-59.
11. Vyas, K.S., et al., *Exosomes: the latest in regenerative aesthetics*. 2023. **18**(2): p. 181-194.
12. Nagelkerke, A., et al., *Extracellular vesicles for tissue repair and regeneration: Evidence, challenges and opportunities*. Adv Drug Deliv Rev, 2021. **175**: p. 113775.
13. Berumen Sánchez, G., et al., *Extracellular vesicles: mediators of intercellular communication in tissue injury and disease*. Cell Communication and Signaling, 2021. **19**(1): p. 104.
14. Ha, D.H., et al., *Mesenchymal Stem/Stromal Cell-Derived Exosomes for Immunomodulatory Therapeutics and Skin Regeneration*. 2020. **9**(5): p. 1157.
15. Zhang, B., et al., *Mesenchymal Stem Cell-Derived Extracellular Vesicles in Tissue Regeneration*. 2020. **29**: p. 0963689720908500.
16. Kwon, H.H., et al., *Combination Treatment with Human Adipose Tissue Stem Cell-derived Exosomes and Fractional CO<sub>2</sub> Laser for Acne Scars: A 12-week Prospective, Double-blind, Randomized, Split-face Study*. Acta Derm Venereol, 2020. **100**(18): p. adv00310.
17. Proffer, S.L., et al., *Efficacy and Tolerability of Topical Platelet Exosomes for Skin Rejuvenation: Six-Week Results*. Aesthet Surg J, 2022. **42**(10): p. 1185-1193.
18. Bataillon, M., et al., *Characterization of a New Reconstructed Full Thickness Skin Model, T-Skin™, and its Application for Investigations of Anti-Aging Compounds*. Int J Mol Sci, 2019. **20**(9).
19. Welsh, J.A., et al., *Minimal information for studies of extracellular vesicles (MISEV2023): From basic to advanced approaches*. 2024. **13**(2): p. e12404.
20. Xu, P., et al., *Extracellular vesicles from adipose-derived stem cells ameliorate ultraviolet B-induced skin photoaging by attenuating reactive oxygen species production and inflammation*. Stem Cell Research & Therapy, 2020. **11**(1): p. 264.
21. Tsai, S.C., et al., *Umbilical Cord Mesenchymal Stromal Cell-Derived Exosomes Rescue the Loss of Outer Hair Cells and Repair Cochlear Damage in Cisplatin-Injected Mice*. Int J Mol Sci, 2021. **22**(13).
22. Pomatto, M., et al., *Differential Therapeutic Effect of Extracellular Vesicles Derived by Bone Marrow and Adipose Mesenchymal Stem Cells on Wound Healing of Diabetic Ulcers and Correlation to Their Cargoes*. Int J Mol Sci, 2021. **22**(8).
23. Michelet, J.F., et al., *The anti-ageing potential of a new jasmonic acid derivative (LR2412): in vitro evaluation using reconstructed epidermis Episkin™*. Exp Dermatol, 2012. **21**(5): p. 398-400.
24. Li, X., et al., *Inflammation and aging: signaling pathways and intervention therapies*. Signal Transduct Target Ther, 2023. **8**(1): p. 239.
25. Marofi, F., et al., *MSCs and their exosomes: a rapidly evolving approach in the context of cutaneous wounds therapy*. Stem Cell Research & Therapy, 2021. **12**(1): p. 597.
26. Janockova, J., et al., *New therapeutic approaches of mesenchymal stem cells-derived exosomes*. Journal of Biomedical Science, 2021. **28**(1): p. 39.
27. Almeria, C., et al., *Heterogeneity of mesenchymal stem cell-derived extracellular vesicles is highly impacted by the tissue/cell source and culture conditions*. Cell Biosci, 2022. **12**(1): p. 51.
28. Wang, X., et al., *Recent progress in exosome research: isolation, characterization and clinical applications*. Cancer Gene Therapy, 2023. **30**(8): p. 1051-1065.
29. Gurung, S., et al., *The exosome journey: from biogenesis to uptake and intracellular signalling*. Cell Communication and Signaling, 2021. **19**(1): p. 47.